Structure–Function Analysis of the TssL Cytoplasmic Domain Reveals a New Interaction between the Type VI Secretion Baseplate and Membrane Complexes

Abdelrahim Zoued, Chloé J Cassaro, Eric Durand, Badreddine Douzi, Alexandre España, Christian Cambillau, Laure Journet, E. Cascales

Structure-function analysis of the TssL cytoplasmic domain reveals a new interaction between the Type VI secretion baseplate and membrane complexes.

Abdelrahim Zoued[1,#], Chloé J. Cassaro[1], Eric Durand[1], Badreddine Douzi[2,3,¶], Alexandre P. España[1,†], Christian Cambillau[2,3], Laure Journet[1], and Eric Cascales[1,*]

[1] Laboratoire d'Ingénierie des Systèmes Macromoléculaires (LISM, UMR 7255), Institut de Microbiologie de la Méditerranée (IMM), Aix-Marseille Univ - Centre National de la Recherche Scientifique (CNRS), 31 chemin Joseph Aiguier, 13402 Marseille Cedex 20, France

[2] Architecture et Fonction des Macromolécules Biologiques (AFMB, UMR 6098), Centre National de la Recherche Scientifique (CNRS), Campus de Luminy, Case 932, 13288 Marseille Cedex 09, France.

[3] Architecture et Fonction des Macromolécules Biologiques (AFMB, UMR 6098), Aix-Marseille Univ, Campus de Luminy, Case 932, 13288 Marseille Cedex 09, France.

Present addresses:

[#] Howard Hughes Medical Institute, Brigham and Women's Hospital, Division of Infectious Diseases and Harvard Medical School, Department of Microbiology and Immunobiology, Boston, Massachusetts, USA

[¶] Laboratoire d'Ingénierie des Systèmes Macromoléculaires (LISM, UMR 7255), Institut de Microbiologie de la Méditerranée (IMM), Aix-Marseille Univ - Centre National de la Recherche Scientifique (CNRS), 31 chemin Joseph Aiguier, 13402 Marseille Cedex 20, France.

[†] Technological Advances for Genomics and Clinics laboratory (TAGC, U1090), Aix-Marseille Univ. - Institut National de la Santé et de la Recherche Médicale (INSERM), 163 Avenue de Luminy, 13288 Marseille Cedex 09, France.

[*]corresponding author: cascales@imm.cnrs.fr

Running head: TssL structure-function analysis

Abstract

The Type VI secretion system (T6SS) is a multiprotein complex that delivers toxin effectors in both prokaryotic and eukaryotic cells. It is constituted of a long cytoplasmic structure - the tail - made of stacked Hcp hexamers and wrapped by a contractile sheath. Contraction of the sheath propels the inner tube capped by the VgrG spike protein towards the target cell. This tubular structure is built onto an assembly platform - the baseplate - that is composed of the TssEFGK-VgrG subunits. During the assembly process, the baseplate is recruited to a trans-envelope complex comprising the TssJ outer membrane lipoprotein and the TssL and TssM inner membrane proteins. This membrane complex serves as docking station for the baseplate/tail and as channel for the passage of the inner tube during sheath contraction. The baseplate is recruited to the membrane complex through multiple contacts including interactions of TssG and TssK with the cytoplasmic loop of TssM, and TssK interaction with the cytoplasmic domain of TssL, $TssL_{Cyto}$. Here, we show that $TssL_{Cyto}$ interacts also with the TssE baseplate subunit. Based on the available $TssL_{Cyto}$ structures, we targeted conserved regions and specific features of $TssL_{Cyto}$ in enteroaggregative *Escherichia coli* (EAEC). By using bacterial two-hybrid and co-immunoprecipitation, we further show that the disordered L3-L4 loop is necessary to interact with TssK, that the L6-L7 loop mediates the interaction with TssE, whereas the TssM cytoplasmic loop binds the conserved groove of $TssL_{Cyto}$. Finally, competition assays demonstrated that these interactions are physiologically important for EAEC T6SS function.

Keywords: Type VI secretion, protein-protein interaction, membrane complex, baseplate complex, loops, crevice, cleft.

Introduction

Bacteria have evolved strategies to survive within difficult environment or to efficiently colonize a specific niche. When nutrients become limiting or when conditions are defavorable, most Gram-negative Proteobacteria delivers anti-bacterial toxins into competitors. One of the main mechanisms for toxin delivery into prokaryotic cells is a multiprotein machinery called Type VI secretion system (T6SS).[1-6] The T6SS resembles a ~ 600-nm long cytoplasmic tail-like tubular structure anchored to the cell envelope, and works as a nano-crossbow.[2,7,8] The T6SS tail shares structural and functional homologies with contractile tail particles such as R-pyocins or bacteriophages.[7-10] The cytoplasmic tubular structure is constituted of an inner tube made of stacked Hcp hexamers organized head-to-tail and wrapped by a contractile sheath.[7,9,11-17] Contraction of the sheath propels the inner tube towards the target cell, allowing toxin delivery and target cell lysis.[7,18-20] This tubular structure is tipped by a spike, composed of a trimer of the VgrG protein and of the PAAR protein, which serves as puncturing device for penetration inside the target cell.[9,21] Toxin effectors are preloaded and different mechanisms of transport have been proposed, including cargo models in which effectors directly or indirectly binds on VgrG, PAAR or within the lumen of Hcp hexamers.[3,6,21-29]

The T6SS tail polymerizes on an assembly platform or baseplate complex (BC), which is also broadly conserved in contractile particles.[30-34] The composition of the T6SS baseplate has been recently revealed and is constituted of five proteins: TssE, TssF, TssG and TssK that assemble a complex together with the VgrG spike.[32,33,35] Once assembled in the cytoplasm, the BC is recruited and stabilized by a trans-envelope complex, or membrane complex (MC), constituted of TssJ, TssL and TssM subunits.[32,36,37] The structure and assembly of the MC are well known. TssJ is an outer membrane lipoprotein with a transthyretin fold[38,39], whereas TssM and TssL are both anchored to the inner membrane. TssM is constituted of three trans-membrane helices (TMH) that delimitate a cytoplasmic loop between TMH2 and TMH3 and a large periplasmic domain downstream TMH3.[40] This periplasmic domain could be segmented into four sub-domains, the C-terminal one mediating contacts with TssJ.[37,39] By contrast, TssL has a single TMH located at its extreme C-terminus, and thus the majority of the protein protrudes into the cytoplasm.[41] The structures of the TssL cytoplasmic domains of enteroaggregative *E. coli* (EAEC), *Francisella tularensis* and *Vibrio cholerae* have been reported: they are composed of 7 helices grouped in two bundles, with an overall shape

resembling a hook.[42-44] The biogenesis of the MC starts with TssJ at the outer membrane and progresses with the sequential addition of TssM and TssL.[37] Ten copies of this heterotrimeric complex then combine to assemble a 1.7-MDa trans-envelope complex that serves both as docking station for the BC/tail structure and as channel for the passage of the inner tube during sheath contraction.[32,37,45] Recruitment of the BC to the MC is mediated by multiple interactions including interactions of TssG and TssK with the cytoplasmic domain of TssM, and of TssK with the cytoplasmic domain of TssL.[32,46]

Here, we conducted a structure-function analysis of the TssL cytoplasmic domain, $TssL_{Cyto}$. We first demonstrate that, in addition to making contacts with the cytoplasmic domain of TssM and TssK, $TssL_{Cyto}$ interacts with the TssE baseplate component. Comparison of the EAEC, *F. tularensis* and *V. cholerae* $TssL_{Cyto}$ structures highlighted the presence of a cleft at the interface of the two-helix bundles with conserved negative charges. In addition, the two loops connecting helices 3-4 and 6-7 display significantly different shapes and/or flexibility. Site-directed mutagenesis coupled to protein-protein interaction studies demonstrated that the L3-4 and L6-7 loops mediate contact with the baseplate components TssK and TssE respectively, whereas the central cleft accommodates the TssM cytoplasmic domain. Finally, anti-bacterial assays showed that all these contacts are necessary for proper function of the Type VI secretion apparatus.

Results

The TssL cytoplasmic domain, $TssL_{Cyto}$, interacts with itself, the cytoplasmic loop of TssM and the TssE and TssK baseplate components.

Previous studies have demonstrated that the cytoplasmic domain of the enteroaggregative *Escherichia coli* TssL protein (EC042_4527; Genbank accession (GI): **284924248**) forms dimers and interacts with the TssM and TssK proteins.[40,42,46] To gain further insights onto the interaction network of $TssL_{Cyto}$, we performed a systematic bacterial two-hybrid (BACTH) analysis (Fig. 1A). As previously shown, we detected $TssL_{Cyto}$ interaction with itself, with TssK and with the cytoplasmic domain of TssM, $TssM_{Cyto}$. In addition, this analysis revealed the interaction between $TssL_{Cyto}$ and the baseplate component TssE (Fig. 1A). The $TssL_{Cyto}$-TssE interaction was further validated *in vitro* by using Surface Plasmon Resonance using purified proteins. TssE was covalently bound to the sensorchip and recordings were monitored after injection of increasing concentrations of $TssL_{Cyto}$ (Fig. 1B

and 1C). The sensorgrams confirmed the BACTH results and demonstrated that the two proteins interact with an affinity estimated to 55 ± 1.3 μM (Fig. 1B and 1C).

Structure analyses of TssL cytoplasmic domains.

The crystal structures of the EAEC, *F. tularensis* and *V. cholerae* TssL cytoplasmic domains are available (PDB IDs: **3U66**[42], **4ACL**[43] and **4V3I**[44]). All structures share common features (Fig. 2A; Supplementary Fig. S1): $TssL_{Cyto}$ is composed of 7 α-helices organized in two bundles constituted of helices α1-4 and α5-7. The α5-7 bundle is made of shorter helices in average, making an overall hook-like structure delimiting a cleft comprising conserved charged residues including aspartate 74 and glutamate 75 (Supplementary Fig. S1A). However, the three structures also highlighted significant differences, notably in loops L3-L4 and L6-L7. $TssL_{Cyto}$ loop L3-L4 is disordered in *F. tularensis* whereas comprises a small additional α-helix, αA, in EAEC and *V. cholerae*. In addition, part of the L3-L4 loop structure could not be solved in the EAEC $TssL_{Cyto}$, suggesting that this loop exhibits structural flexibility. $TssL_{Cyto}$ loop L6-L7 comprises an additional α-helix, αB, in *V. cholerae*, whereas adopts different conformations in EAEC and *F. tularensis* (Supplementary Fig. S1). These two loops having distinct structures, conformations or flexibility, they could be considered as interesting binding sites to confer specificity.

Mutagenesis of the charged cleft and L3-L4 and L6-L7 loops unveils contact zones with $TssM_{Cyto}$, TssK and TssE.

To gain information on the role of the conserved cleft and of the L3-L4 and L6-L7 loops, we engineered amino-acid substitutions in these different regions (Fig. 2B and Table 1): (i) two charged residues (Glu-81 and Asp-84) within loop L3-L4 were converted to opposed charges (GluAsp-to-LysLys mutant, called hereafter EKDK) (orange arrows in Fig. 2), (ii) small (Gly-137), aromatic (Phe-138) and charged (Asp-74 and Glu-75) chains within the cleft were substituted to yield Gly-to-Glu (GE), Phe-to-Glu (FE), GlyPhe-to-GluGlu (GEFE), Asp-to-Arg (DR), Glu-to-Arg (ER) and AspGlu-to-ArgArg (DRER) mutants (green arrows in Fig. 2), and (iii) three hydrophilic/charged residues within loop L6-L7 (Gln-145,

Asp-146 and Asp-147) were substituted with Lysine residues (GlnAspAsp-to-LysLysLys, QKDKDK) (blue arrows in Fig. 2).

These substitutions were first introduced into the $TssL_{Cyto}$-T18 and pIBA-$TssL_{Cyto}$ vectors to test their impact on the interaction with TssE, TssK and the cytoplasmic loop of TssM, $TssM_{Cyto}$, using bacterial two-hybrid and co-immunoprecipitation (Fig. 3). Two-hybrid analyses showed that none of these substitutions break the oligomerization of $TssL_{Cyto}$ (Fig. 3A), in agreement with a previous study showing that $TssL_{Cyto}$ oligomerization is mediated by contacts between helices α1.[42] These results also suggest that each mutant variant is properly produced and does not present large structural changes compared to the wild-type $TssL_{Cyto}$ domain. The assay also revealed that most mutations within the $TssL_{Cyto}$ central cleft prevent formation of the $TssL_{Cyto}$- $TssM_{Cyto}$ complex whereas substitutions within loops L3-L4 and L6-L7 abolish interaction with TssK and TssE, respectively (Fig. 3A).

These two-hybrid results were validated by co-immuno-precipitation analyses. Soluble lysates of cells producing the C-terminally FLAG-tagged wild-type TssL cytoplasmic domain and its substitution variants were combined with lysates containing VSV-G-tagged TssE, TssK and $TssM_{Cyto}$. $TssL_{Cyto}$-containing complexes were immobilized on agarose beads coupled to the monoclonal anti-FLAG antibody. Figure 3B shows that the wild-type $TssL_{Cyto}$ domain co-precipitates TssE, TssK and $TssM_{Cyto}$. Each $TssL_{Cyto}$ variant is produced and immuno-precipitated at levels comparable to the wild-type $TssL_{Cyto}$ domain. Mutation of the Glu-Asp (EKDK mutant) and Gln-Asp-Asp (QKDKDK mutant) motifs within the L3-L4 and L6-L7 loops prevented interaction with TssK and TssE respectively, whereas most substitutions within the conserved groove abolished interaction with the TssM cytoplasmic domain (Fig. 3B).

$TssL_{Cyto}$ interactions with TssE, TssK and $TssM_{Cyto}$ are critical for proper function of the Type VI secretion apparatus.

The EAEC Sci-1 T6SS is involved in inter-bacterial competition by delivering Tle1, a toxin with phospholipase activity into competitor cells.[27] We therefore tested whether substitutions that abolish $TssL_{Cyto}$ complexes formation impact the function of the T6SS. The substitutions were introduced into the pOK-TssL vector, that encodes the full length TssL protein and previously shown to fully complement the Δ*tssL* phenotypes.[41] The anti-bacterial

activity was tested against a competitor strain engineered to constitutively express the GFP and to resist kanamycin. The fluorescence levels of mixture containing the EAEC and competitor strains at a 4:1 ratio, which is proportional to the number of competitor cells was measured after 4 hours of contact. In addition, the survival of the competitor strain was measured by counting fluorescent colony-forming units (cfu) after plating serial dilutions of the mixture on plates supplemented with kanamycin. The results represented in Figure 4 show that the growth of the competitor strain was inhibited by the Δ*tssL* strain producing the wild-type TssL protein, at a level comparable to that of the wild-type strain. By contrast, the Δ*tssL* strain did not cause growth inhibition of competitor cells. With the exception of the FE mutant strain, all the TssL variants were unable to complement the anti-bacterial defects of the Δ*tssL* strain, demonstrating the formation of $TssL_{Cyto}$-TssE, $TssL_{Cyto}$-TssK and $TssL_{Cyto}$-$TssM_{Cyto}$ complexes is necessary for proper assembly and function of the EAEC Sci-1 T6SS.

Discussion

In this study, we have used a systematic bacterial two-hybrid approach to define the partners of the T6SS TssL cytoplasmic domain. In addition to the known interacting subunits, TssM[40] and TssK[46], we have found an additional contact with the TssE protein, a component of the baseplate. This interaction was confirmed *in vitro* using surface plasmon resonance. With the identification of $TssM_{Cyto}$-TssG, $TssM_{Cyto}$-TssK and $TssL_{Cyto}$-TssK contacts[32,46,47], the interaction of $TssL_{Cyto}$ with TssE corresponds to the fourth interaction between the T6SS membrane and baseplate complex. The cytoplasmic domain of TssL is located at the base of the TssJLM complex[37], a location compatible with the position of the baseplate *in vivo*.[7,32,48] Although these interactions are of low affinity between isolated molecules (the dissociation constant measured *in vitro* for the $TssL_{Cyto}$-TssE interaction is ~ 50 µM), the avidity should increase within the secretion apparatus by the number of interactions and the local concentration. Furthermore, the existence of four contacts likely stabilizes the recruitment of the baseplate to the membrane complex. These multiple contacts are probably important to properly position the baseplate onto the membrane complex and to maintain the baseplate stably anchored when the sheath contracts. In addition, it has been shown that the bacteriophage T4 baseplate is subjected to large conformational changes during sheath contraction[33,49], and a similar situation is likely to occur in the case of the T6SS.[30,32] Therefore

it might be critical to have a multitude of contacts between the baseplate and membrane complexes as several interactions might be broken during the conformational transition.

TssL dimerizes and interacts with three proteins of the secretion apparatus (Fig. 5). In enteroaggregative *E. coli*, TssL dimerization occurs mainly by the trans-membrane segment with contribution of residues from helix α1. In this study, we provided further molecular details on the TssL interaction by conducting a structure-function analysis. First, using sequence alignment, we defined that a number of residues share high level of conservation. Interestingly, most of these residues locate at the interface between the two-helix bundles and delimitate a cleft. Second, by comparing the three available crystal structures of TssL cytoplasmic domains (from EAEC, *F. tularensis* and *V. cholerae*), we targeted two loops, loops L3-L4 and L6-L7, which present different shapes, distinct secondary structures (addition of short helices) and are highly degenerated. Substitutions were introduced in the cleft as well as in loops L3-L4 and L6-L7 and were tested for their impact on the interactions. None of these mutations disrupted the oligomerization of $TssL_{Cyto}$ suggesting that their impact on $TssL_{Cyto}$ folding was null or moderated. Our data show that the cleft is required for proper interaction with $TssM_{Cyto}$, whereas loops L3-L4 and L6-L7 are putative binding sites for TssK and TssE respectively. The conservation of the charged crevice in TssL proteins suggests that the mode of binding of TssL/TssM proteins might be conserved. It is worthy to note that the T6SS-associated TssL and TssM proteins share homologies with IcmH/DotU and IcmF, two subunits of the *Legionella pneumophila* Type IVb secretion system (T4bSS).[8,42] Interestingly, IcmH/DotU also possesses charged residues in the putative cleft position, suggesting that this cleft might also be important for binding to IcmF. By contrast, the variability of the L3-L4 and L6-L7 loops might confer specificity between TssL proteins and the baseplate complex, notably when different T6SS are produced simultaneously in a bacterium. However, while our results demonstrate that these regions are necessary for these interactions, it remains to be defined whether these regions are sufficient. Swapping experiments between TssL proteins from different bacteria would be an interesting extension of this study. Finally, these data are interesting for the development of inhibitors that will target the assembly of the membrane complex or the recruitment of the baseplate. Specifically, crevices such as the cleft that accommodates the TssM cytoplasmic domain are interesting targets for drugs, while mimetic peptides might be used to prevent interaction of the baseplate components with the TssL loops.

MATERIALS and METHODS

Bacterial strains and media. The *Escherichia coli* K-12 DH5α, BTH101, W3110 and BL21(DE3) pLysS strains were used for cloning procedures, bacterial two-hybrid analyses, co-immunoprecipitations and protein production, respectively. Strain W3110 pUA66-*rrnB* (Kan^R, constitutively expressing the Green Fluorescent Protein [GFP])[50,51] was used as prey in anti-bacterial competition experiments. Enteroaggregative *E. coli* (EAEC) strain 17-2 has been used as source of DNA for PCR amplification, and for phenotypic analyses. The Δ*tssL* 17-2 derivative mutant strain has been previously described.[36] Cells were grown in Lysogeny broth (LB), Terrific Broth (TB) or Sci-1-inducing medium (SIM)[52] as specified. Plasmids were maintained by the addition of ampicillin (100 µg/mL), chloramphenicol (40 µg/mL) or kanamycin (50 µg/mL for *E. coli* K-12 and 100 µg/mL for EAEC). Expression of genes cloned into pOK12, pASK-IBA37+, pBAD33 and pETG20A vectors were induced by the addition of isopropyl-thio-β-D-galactopyrannoside (IPTG; 50 µM in liquid, 10 µM on agar plates), anhydrotetracyclin (AHT; 0.1 µg/mL), L-arabinose (0.2%) and IPTG (0.5 mM), respectively.

Plasmid construction. Plasmids used in this study are listed in Supplemental Table S1. Polymerase Chain Reactions (PCR) were performed using a Biometra thermocycler using the Q5 high fidelity DNA polymerase (New England BioLabs). Custom oligonucleotides, listed in Supplemental Table S1, were synthesized by Sigma Aldrich. Enteroaggregative *E. coli* 17-2 chromosomal DNA was used as a template for all PRCs. The amplified DNA fragments correspond to the full-length or the cytoplasmic domain ($TssL_{Cyto}$, residues 1-184)[41] of TssL (EC042_4527, GI: 284924248), the full-length TssK (EC042_4526, GI: 284924247) and TssE (EC042_4545, GI: 284924266) proteins, and the cytoplasmic domain ($TssM_{Cyto}$, residues 62-360) of the TssM protein (EC042_4539, GI: 284924260). The pOK-TssL plasmid, producing the full-length TssL proteins fused to a C-terminal HA epitope and plasmids pETG20A-$TssL_{Cyto}$ and pETG20A-TssE have been previously described.[41,42,45] pASK-IBA37+, pBAD33 plasmid derivatives were engineered by restriction-free cloning[53] as previously described.[36] Briefly, genes of interest were amplified with oligonucleotides introducing extensions annealing to the target vector. The double-stranded product of the first PCR was then been used as oligonucleotides for a second PCR using the target vector as template. Codon substitutions have been obtained by site-directed mutagenesis using complementary oligonucleotides bearing the nucleotide modifications. All constructs have been verified by restriction analysis and DNA sequencing (Eurofins, MWG).

Bacterial two-hybrid assay. The adenylate cyclase-based bacterial two-hybrid technique[54] was used as previously published.[55] Briefly, compatible vectors producing proteins fused to the isolated T18 and

T25 catalytic domains of the *Bordetella* adenylate cyclase were transformed into the reporter BTH101 strain and the plates were incubated at 30°C for 24 hours. Three independent colonies for each transformation were inoculated into 600 µL of LB medium supplemented with ampicillin, kanamycin and IPTG (0.5 mM). After overnight growth at 30°C, 10 µL of each culture were spotted onto LB plates supplemented with ampicillin (100 µg/mL), kanamycin (50 µg/mL), IPTG (0.5 mM) and bromo-chloro-indolyl-β-D-galactopyrannoside (40 µg/mL) and incubated for 16 hours at 30 °C. The experiments were done at least in triplicate from independent transformations and a representative result is shown.

Co-immunoprecipitations. W3110 cells producing the protein of interest were grown to an A_{600} ~ 0.4 and the expression of the cloned genes were induced with AHT (0.1 µg/mL) or L-arabinose (0.2%) for 1 hour. 10^{10} cells were harvested, and the pellets were resuspended in 1 mL of LyticB buffer (Sigma-Aldrich) supplemented with lysozyme 100 µg/mL, DNase 100 µg/mL and protease inhibitors (Complete, Roche) and incubated for 20 min at 25°C. Lysates were then clarified by centrifugation at 20,000 × *g* for 10 min. 250 µL of each lysate were mixed, incubated for 30 min on a wheel and the mixture was applied on anti-FLAG M2 affinity gel (Sigma-Aldrich). After 2 hours of incubation, the beads were washed three times with 1 mL of 20 mM Tris-HCl pH 7.5, 100 mM NaCl, resuspended in 25 µL of Laemmli loading buffer, boiled for 10 min and subjected to SDS-PAGE and immunodetection analyses.

Anti-bacterial competition assay. Antibacterial competition growth assays were performed as previously described in Sci-1-inducing conditions[27], except that cultures were supplemented with IPTG 50 µM, and that IPTG (10 µM) was added on the competition plates. The wild-type *E. coli* strain W3110 bearing the kanamycin-resistant GFP^+ pUA66-*rrnB* plasmid[51] was used as prey. After incubation on plates for 4 hours, cells were scratched off and the fluorescence levels were measured using a TECAN infinite M200 microplate reader. The number of surviving prey cells was measured by counting fluorescent colonies on kanamycin plates.

Protein purification. The TssE protein and TssL cytoplasmic domain produced from pETG20A derivatives are fused to an N-terminal 6×His-tagged thioredoxin (TRX) followed by a cleavage site for the Tobacco etch virus (TEV) protease. Purifications of TssE and $TssL_{Cyto}$ have been performed as previously described.[42,45] Briefly, *E. coli* BL21(DE3) pLysS cells carrying the pETG20A plasmid derivatives were grown at 37°C in TB medium (1.2% peptone, 2.4% yeast extract, 72 mM K_2HPO_4, 17 mM KH_2PO_4, and 0.4% glycerol) and expression of the cloned genes was induced at A_{600}= 0.6 with 0.5 mM IPTG for 18 hours at 16°C. Cells were then resuspended in lysis buffer (50 mM Tris-HCl pH 8.0, 300 mM NaCl, 1 mM EDTA, 0.5 mg/mL lysozyme, 1mM phenylmethylsulfonyl fluoride), submitted to four freeze-thawing cycles and sonicated after the addition of 20 µg/mL DNase and 20

mM $MgCl_2$. The soluble fraction obtained after centrifugation for 30 min at 16,000 × *g* was loaded onto a 5-mL Nickel column (HisTrap™ FF) using an ÄKTA Explorer apparatus (GE healthcare) and the immobilized proteins were eluted in 50 mM Tris-HCl pH8.0, 300 mM NaCl supplemented with 250 mM imidazole. The protein solution was desalted on a HiPrep 26/10 column (Sephadex^{TM} G-25, Amersham Biosciences), and untagged proteins were obtained by cleavage using 2 mg of TEV protease for 18 hours at 4°C and collected in the flow-through of a 5-mL Nickel column. The proteins were concentrated using the centricon technology (Millipore, 10-kDa cut-off). After concentration, the soluble proteins were passed through a Sephadex 200 26/60 column pre-equilibrated with 25 mM Tris-HCl pH7.5, 100 mM NaCl, 5% Glycerol.

Surface Plasmon Resonance (SPR). Steady state interactions were monitored by SPR using a BIAcore T200 at 25°C, as previously described.[39] Briefly, the HC200m sensor chip (Xantech) was coated with purified the thioredoxin-TssE fusion protein immobilized by amine coupling (ΔRU=4000-4300). A control flow-cell was coated with thioredoxin immobilized by amine coupling at the same concentration (ΔRU=4100). Purified $TssL_{Cyto}$ (five concentrations ranging from 5 to 75 µM) were injected and binding traces were recorded in duplicate. The signal from the control flow cell and the buffer response were subtracted from all measurements. The dissociation constants (K_D) were estimated using the GraphPad Prism 5.0 software on the basis of the steady state levels of ΔRU, directly related to the concentration of the analytes. The K_D were estimated by plotting the different ΔRU at a fixed time (5 s before the end of the injection step) against the different concentrations of $TssL_{Cyto}$. For K_D calculation, nonlinear regression fit for XY analysis was used and one site (specific binding) as a model which corresponds to the equation Y = Bmax*X/(Kd + X).

References

1. Coulthurst, S. J. (2013). The Type VI secretion system - a widespread and versatile cell targeting system. Res Microbiol.164, 640-654.

2. Zoued, A., Brunet, Y. R., Durand, E., Aschtgen, M. S., Logger, L., Douzi, B., Journet, L., Cambillau, C. & Cascales, E. (2014). Architecture and assembly of the Type VI secretion system. Biochim Biophys Acta. 1843, 1664-1673.

3. Durand, E., Cambillau, C., Cascales, E. & Journet, L. (2014). VgrG, Tae, Tle, and beyond: the versatile arsenal of Type VI secretion effectors. Trends Microbiol. 22, 498-507.

4. Ho, B. T., Dong, T. G. & Mekalanos, J. J. (2014). A view to a kill: the bacterial type VI secretion system. Cell Host Microbe. 15, 9-21.

5. Basler, M. (2015). Type VI secretion system: secretion by a contractile nanomachine. Philos Trans R Soc Lond B Biol Sci. 370, 1679.

6. Alcoforado Diniz, J., Liu, Y. C. & Coulthurst, S. J. (2015). Molecular weaponry: diverse effectors delivered by the Type VI secretion system. Cell Microbiol. 17, 1742-1751.

7. Basler, M., Pilhofer, M., Henderson, G. P., Jensen, G. J. & Mekalanos, J. J. (2012). Type VI secretion requires a dynamic contractile phage tail-like structure. Nature. 483, 182-186.

8. Cascales, E. & Cambillau, C. (2012). Structural biology of type VI secretion systems. Philos Trans R Soc Lond B Biol Sci. 367, 1102-1111.

9. Leiman, P. G., Basler, M., Ramagopal, U. A., Bonanno, J. B., Sauder, J. M., Pukatzki, S., Burley, S. K., Almo, S. C. & Mekalanos, J. J. (2009). Type VI secretion apparatus and phage tail-associated protein complexes share a common evolutionary origin. Proc Natl Acad Sci USA. 106, 4154-4159.

10. Bönemann, G., Pietrosiuk, A. & Mogk, A. (2010). Tubules and donuts: a type VI secretion story. Mol Microbiol. 76, 815-821.

11. Mougous, J. D., Cuff, M. E., Raunser, S., Shen, A., Zhou, M., Gifford, C. A., Goodman, A. L., Joachimiak, G., Ordoñez, C. L., Lory, S., Walz, T., Joachimiak, A. & Mekalanos, J. J. (2006). A virulence locus of Pseudomonas aeruginosa encodes a protein secretion apparatus. Science. 312, 1526-1530.

12. Ballister, E. R., Lai, A. H., Zuckermann, R. N., Cheng, Y. & Mougous, J. D. (2008). In vitro self-assembly of tailorable nanotubes from a simple protein building block. Proc Natl Acad Sci USA. 105, 3733-3738.

13. Lossi, N. S., Manoli, E., Förster, A., Dajani, R., Pape, T., Freemont, P. & Filloux, A. (2013). The HsiB1C1 (TssB-TssC) complex of the Pseudomonas aeruginosa type VI secretion system forms a bacteriophage tail sheathlike structure. J Biol Chem. 288, 7536-7548.

14. Brunet, Y. R., Hénin, J., Celia, H. & Cascales, E. (2014). Type VI secretion and bacteriophage tail tubes share a common assembly pathway. EMBO Rep. 15, 315-321.

15. Douzi, B., Spinelli, S., Blangy, S., Roussel, A., Durand, E., Brunet, Y. R., Cascales, E. & Cambillau, C. (2014). Crystal structure and self-interaction of the type VI secretion tail-tube protein from enteroaggregative Escherichia coli. PLoS One. 9, e86918.

16. Zhang, X. Y., Brunet, Y. R., Logger, L., Douzi, B., Cambillau, C., Journet, L. & Cascales, E. (2013). Dissection of the TssB-TssC interface during type VI secretion sheath complex formation. PLoS One. 8, e81074.

17. Kudryashev, M., Wang, R. Y., Brackmann, M., Scherer, S., Maier, T., Baker, D., DiMaio, F., Stahlberg, H., Egelman, E. H. & Basler, M. (2015). Structure of the type VI secretion system contractile sheath. Cell. 160, 952-962.

18. LeRoux, M., De Leon, J. A., Kuwada, N. J., Russell, A. B., Pinto-Santini, D., Hood, R. D., Agnello, D. M., Robertson, S. M., Wiggins, P. A. & Mougous, J. D. (2012). Quantitative single-cell characterization of bacterial interactions reveals type VI secretion is a double-edged sword. Proc Natl Acad Sci USA. 109, 19804-19809.

19. Basler, M., Ho, B. T. & Mekalanos, J. J. (2013). Tit-for-tat: type VI secretion system counterattack during bacterial cell-cell interactions. Cell. 152, 884-894.

20. Brunet, Y. R., Espinosa, L., Harchouni, S., Mignot, T. & Cascales, E. (2013). Imaging type VI secretion-mediated bacterial killing. Cell Rep. 3, 36-41.

21. Shneider, M. M., Buth, S. A., Ho, B. T., Basler, M., Mekalanos, J. J. & Leiman, P. G. (2013). PAAR-repeat proteins sharpen and diversify the type VI secretion system spike. Nature. 500, 350-353.

22. Pukatzki, S., Ma, A. T., Revel, A. T., Sturtevant, D. & Mekalanos, J. J. (2007). Type VI secretion system translocates a phage tail spike-like protein into target cells where it cross-links actin. Proc Natl Acad Sci USA. 104, 15508-15513.

23. Silverman, J. M., Agnello, D. M., Zheng, H., Andrews, B. T., Li, M., Catalano, C. E., Gonen, T. & Mougous, J. D. (2013). Haemolysin coregulated protein is an exported receptor and chaperone of type VI secretion substrates. Mol Cell. 51, 584-593.

24. Alcoforado Diniz, J., Liu, Y. C. & Coulthurst, S. J. (2015). Molecular weaponry: diverse effectors delivered by the Type VI secretion system. Cell Microbiol. 17, 1742-1751.

25. Unterweger, D., Kostiuk, B., Ötjengerdes, R., Wilton, A., Diaz-Satizabal, L. & Pukatzki, S. (2015). Chimeric adaptor proteins translocate diverse type VI secretion system effectors in Vibrio cholerae. EMBO J. 34, 2198-2210.

26. Liang, X., Moore, R., Wilton, M., Wong, M. J., Lam, L. & Dong, T. G. (2016). Identification of divergent type VI secretion effectors using a conserved chaperone domain. Proc Natl Acad Sci USA. 112, 9106-9111.

27. Flaugnatti, N., Le, T. T., Canaan, S., Aschtgen, M. S., Nguyen, V. S., Blangy, S., Kellenberger, C., Roussel, A., Cambillau, C., Cascales, E. & Journet, L. (2016). A phospholipase A1 anti-bacterial T6SS effector interacts directly with the C-terminal domain of the VgrG spike protein for delivery. Mol Microbiol. 99, 1099-1118.

28. Bondage, D. D., Lin, J. S., Ma, L. S., Kuo, C. H. & Lai, E. M. (2016). VgrG C terminus confers the type VI effector transport specificity and is required for binding with PAAR and adaptor-effector complex. Proc Natl Acad Sci USA. 113, 3931-3940.

29. Cianfanelli, F. R., Alcoforado Diniz, J., Guo, M., De Cesare, V., Trost, M. & Coulthurst, S. J. (2016). VgrG and PAAR proteins define distinct versions of a functional Type VI secretion system. PLoS Pathog. 12, e1005735.

30. Leiman, P. G. & Shneider, M. M. (2012). Contractile tail machines of bacteriophages. Adv Exp Med Biol. 726, 93-114.

31. Sarris, P. F., Ladoukakis, E. D., Panopoulos, N. J. & Scoulica, E. V. (2014). A phage tail-derived element with wide distribution among both prokaryotic domains: a comparative genomic and phylogenetic study. Genome Biol Evol. 6, 1739-1747.

32. Brunet, Y. R., Zoued, A., Boyer, F., Douzi, B. & Cascales, E. (2015). The Type VI secretion TssEFGK-VgrG phage-like baseplate is recruited to the TssJLM membrane complex via multiple contacts and serves as assembly platform for tail tube/sheath polymerization. PLoS Genet. 11, e1005545.

33. Taylor, N. M., Prokhorov, N. S., Guerrero-Ferreira, R. C., Shneider, M. M., Browning, C., Goldie, K. N., Stahlberg, H. & Leiman, P. G. (2016). Structure of the T4 baseplate and its function in

triggering sheath contraction. Nature. 533, 346-352.

34. Filloux, A. & Freemont, P. (2016). Structural biology: baseplates in contractile machines. Nat Microbiol. in press.

35. English, G., Byron, O., Cianfanelli, F. R., Prescott, A. R. & Coulthurst, S. J. (2014). Biochemical analysis of TssK, a core component of the bacterial Type VI secretion system, reveals distinct oligomeric states of TssK and identifies a TssK-TssFG subcomplex. Biochem J. 461, 291-304.

36. Aschtgen, M. S., Gavioli, M., Dessen, A., Lloubès, R. & Cascales, E. (2010). The SciZ protein anchors the enteroaggregative Escherichia coli Type VI secretion system to the cell wall. Mol Microbiol. 75, 886-899.

37. Durand, E., Nguyen, V. S., Zoued, A., Logger, L., Péhau-Arnaudet, G., Aschtgen, M. S., Spinelli, S., Desmyter, A., Bardiaux, B., Dujeancourt, A., Roussel, A., Cambillau, C., Cascales, E. & Fronzes, R. (2015). Biogenesis and structure of a type VI secretion membrane core complex. Nature. 523, 555-560.

38. Aschtgen, M. S., Bernard, C. S., De Bentzmann, S., Lloubès, R. & Cascales, E. (2008). SciN is an outer membrane lipoprotein required for type VI secretion in enteroaggregative Escherichia coli. J Bacteriol. 190, 7523-7531.

39. Felisberto-Rodrigues, C., Durand, E., Aschtgen, M. S., Blangy, S., Ortiz-Lombardia, M., Douzi, B., Cambillau, C. & Cascales, E. (2011). Towards a structural comprehension of bacterial type VI secretion systems: characterization of the TssJ-TssM complex of an Escherichia coli pathovar. PLoS Pathog. 7, e1002386.

40. Ma, L. S., Lin, J. S. & Lai, E. M. (2009). An IcmF family protein, ImpLM, is an integral inner membrane protein interacting with ImpKL, and its walker a motif is required for type VI secretion system-mediated Hcp secretion in Agrobacterium tumefaciens. J Bacteriol. 191, 4316-4129.

41. Aschtgen, M. S., Zoued, A., Lloubès, R., Journet, L. & Cascales, E. (2012). The C-tail anchored TssL subunit, an essential protein of the enteroaggregative Escherichia coli Sci-1 Type VI secretion system, is inserted by YidC. Microbiologyopen. 1, 71-82.

42. Durand, E., Zoued, A., Spinelli, S., Watson, P. J., Aschtgen, M. S., Journet, L., Cambillau, C. & Cascales, E. (2012). Structural characterization and oligomerization of the TssL protein, a component shared by bacterial type VI and type IVb secretion systems. J Biol Chem. 287, 14157-14168.

43. Robb, C. S., Nano, F. E. & Boraston, A. B. (2012). The structure of the conserved type six secretion protein TssL (DotU) from Francisella novicida. J Mol Biol. 419, 277-283.

44. Chang, J. H. & Kim, Y. G. (2015). Crystal structure of the bacterial type VI secretion system component TssL from Vibrio cholerae. J Microbiol. 53, 32-37.

45. Zoued, A., Durand, E., Brunet, Y. R., Spinelli, S., Douzi, B., Guzzo, M., Flaugnatti, N., Legrand, P., Journet, L., Fronzes, R., Mignot, T., Cambillau, C. & Cascales, E. (2016). Priming and polymerization of a bacterial contractile tail structure. Nature. 531, 59-63.

46. Zoued, A., Durand, E., Bebeacua, C., Brunet, Y. R., Douzi, B., Cambillau, C., Cascales, E. & Journet, L. (2013). TssK is a trimeric cytoplasmic protein interacting with components of both

phage-like and membrane anchoring complexes of the type VI secretion system. J Biol Chem. 288, 27031-27041.

47. Logger, L., Aschtgen, M. S., Guérin, M., Cascales, E. & Durand, E. (2016). Molecular dissection of the interface between the Type VI secretion TssM cytoplasmic domain and the TssG baseplate component. J Mol Biol

48. Gerc, A. J., Diepold, A., Trunk, K., Porter, M., Rickman, C., Armitage, J. P., Stanley-Wall, N. R. & Coulthurst, S. J. (2015). Visualization of the Serratia Type VI secretion system reveals unprovoked attacks and dynamic assembly. Cell Rep. 12, 2131-2142.

49. Kostyuchenko, V. A., Leiman, P. G., Chipman, P. R., Kanamaru, S., van Raaij, M. J., Arisaka, F., Mesyanzhinov, V. V. & Rossmann, M. G. (2003). Three-dimensional structure of bacteriophage T4 baseplate. Nat Struct Biol. 10, 688-693.

50. Gueguen, E. & Cascales, E. (2013). Promoter swapping unveils the role of the Citrobacter rodentium CTS1 type VI secretion system in interbacterial competition. Appl Environ Microbiol. 79, 32-38.

51. Zaslaver, A., Bren, A., Ronen, M., Itzkovitz, S., Kikoin, I., Shavit, S., Liebermeister, W., Surette, M. G. & Alon, U. (2006). A comprehensive library of fluorescent transcriptional reporters for Escherichia coli. Nat Methods. 3, 623-628.

52. Brunet, Y. R., Bernard, C. S., Gavioli, M., Lloubès, R. & Cascales, E. (2011). An epigenetic switch involving overlapping fur and DNA methylation optimizes expression of a type VI secretion gene cluster. PLoS Genet. 7, e1002205.

53. van den Ent, F. & Löwe, J. (2006). RF cloning: a restriction-free method for inserting target genes into plasmids. J Biochem Biophys Methods. 67, 67-74.

54. Karimova, G., Pidoux, J., Ullmann, A. & Ladant, D. (1998). A bacterial two-hybrid system based on a reconstituted signal transduction pathway. Proc Natl Acad Sci USA. 95, 5752-5756.

55. Battesti, A. & Bouveret, E. (2012). The bacterial two-hybrid system based on adenylate cyclase reconstitution in Escherichia coli. Methods. 58, 325-334.

56. Pettersen, E. F., Goddard, T. D., Huang, C. C., Couch, G. S., Greenblatt, D. M., Meng, E. C. & Ferrin, T. E. (2004). UCSF Chimera - a visualization system for exploratory research and analysis. J Comput Chem. 25, 1605-1612.

Acknowledgements

We thank Laetitia Houot and Bérengère Ize and the members of the Cascales, Cambillau, Lloubès, Bouveret and Sturgis research groups for insightful discussions, Annick Brun, Isabelle Bringer and Olivier Uderso for technical assistance, and Marc Assin for encouragements. This work was supported by the Centre Nationale de la Recherche Scientifique (CNRS), the Aix-Marseille Université (AMU) and Agence Nationale de la Recherche (ANR) and Fondation pour la Recherche Médicale (FRM) research grants (ANR-

10-JCJC-1303-03, ANR-14-CE14-0006-02, DEQ2011-0421282). A.Z. was a recipient of a Ministère de la Recherche doctoral and FRM end-of-thesis (FDT20140931060) fellowships.

Authors contribution

A.Z., A.E. and L.J. constructed the vectors for the *in vivo* studies and performed the BACTH experiments, Chl.C. performed the co-immunoprecipitations and anti-bacterial assays, A.Z., E.D. and E.C. analysed the TssL structure and identified regions for mutagenesis, B.D. purified TssE and performed SPR experiments E.C. and C.C. supervised the experiments. E.C. wrote the manuscript. Each author reviewed the manuscript prior to submission.

Additional information

Supplemental information. The supplemental information contains one Supplemental Table (Strains, Plasmids and Oligonucleotides used in this study) and two Supplemental Figure (S1, Comparison of the EAEC, *F. tularensis* and *V. cholerae* $TssL_{Cyto}$ structures; S2, Sequence alignment of TssL proteins).

Competing financial interests. The authors declare no competing financial interests.

Legend to Figures

Figure 1. **$TssL_{Cyto}$ oligomerizes and interacts with TssE, TssK and $TssM_{Cyto}$. (A)** Bacterial two-hybrid assay. BTH101 reporter cells producing the $TssL_{Cyto}$-T18 fusion protein and the indicated T6SS proteins fused to the T25 domain of the *Bordetella* adenylate cyclase were spotted on X-Gal-IPTG reporter LB agar plates. Only the cytoplasmic (Cyto) or periplasmic (Peri) domains were used for membrane-anchored proteins. **(B** and **C)** Surface plasmon resonance analysis. SPR sensorgrams (expressed as variation of resonance units, ΔRU) were recorded after injection of the increasing concentrations of purified $TssL_{Cyto}$ (from light grey to black: 5, 10, 20, 37.5 and 75 µM) on TssE-coated HC200m chips (**B**). The graphes reporting ΔRU as a function of $TssL_{Cyto}$ concentration were used to estimate the dissociation constants of the $TssL_{Cyto}$-TssE complex (**C**).

Figure 2. Structure of the EAEC $TssL_{Cyto}$ domain. (A) Crystal structure of the EAEC $TssL_{Cyto}$ domain. The protein is shown as ribbon and α-helices (α1-α7) are indicated. The unstructured L3-L4 loop (orange arrow) is shown in dotted line, whereas the L6-L7 loop and the cleft are indicated by blue and green arrows respectively. The figure was made with Chimera.[56] (**B**) Sequence of the crystallized $TssL_{Cyto}$ domain, with the same color code that in panel A. The residues substituted in this study are indicated by arrowheads (green, cleft; orange, L3-L4 loop; blue, L6-L7 loop).

Figure 3. Distinct motifs on $TssL_{Cyto}$ mediate interactions with TssE, TssK and $TssM_{Cyto}$ (**A**) Bacterial two-hybrid assay. BTH101 reporter cells producing the $TssL_{Cyto}$-T18 fusion protein variants and the indicated T6SS proteins fused to the T25 domain of the *Bordetella* adenylate cyclase were spotted on X-Gal-IPTG reporter LB agar plates. Only the cytoplasmic (*c*) or periplasmic (*p*) domains were used for membrane-anchored proteins. (**B**) Co-immunoprecipitation assay. Soluble lysates from 3×10^{10} *E. coli* K12 W3110 cells producing WT or mutant FLAG-tagged $TssL_{Cyto}$ (Lc_{FL}) and VSV-G-tagged TssE ($TssE_V$), TssK ($TssK_V$) or $TssM_{Cyto}$ ($TssMc_V$) proteins were subjected to immunoprecipitation with anti-FLAG-coupled beads. The lysates and immunoprecipitated (IP) material were separated by 12.5% acrylamide SDS-PAGE and immunodetected with anti-FLAG (lower panels) and anti-VSV-G (upper panels) monoclonal antibodies. Molecular weight markers (in kDa) are indicated.

Figure 4. $TssL_{Cyto}$ interactions with TssE, TssK and $TssM_{Cyto}$ are required for T6SS anti-bacterial activity. *E. coli* K-12 prey cells (W3110 gfp^+, kan^R) were mixed with the indicated attacker cells, spotted onto Sci-1 inducing medium (SIM) agar plates and incubated for 4 hours at 37°C. The relative fluorescence of the bacterial mixture (in arbitrary unit, AU) is indicated in the upper graph, and the number of recovered *E. coli* prey cells (counted on selective kanamycin medium) is indicated in the graph (in log10 of colony-forming unit (cfu)). The circles indicate values from three

independent assays, and the average is indicated by the bar.

Figure 5. Schematic representation of the $TssL_{Cyto}$ interaction network. Schematic representation of the TssJLM membrane complex (MC) and its interactions with the TssKEFG-VgrG baseplate complex (BC). The TssL ($TssL_{Cyto}$) and TssM ($TssM_{Cyto}$) cytoplasmic domains are shown in orange and blue respectively. The interactions defined in this study are indicated by red arrows. Interactions determined previously[46] or in the accompanying article[47] are shown in blue dashed arrows.

Legend to Supplementary Data

Figure S1. Comparison of the three available $TssL_{Cyto}$ crystal structures. (**A**) Sequence alignement of the enteroaggregative *E. coli* (EAEC), *Francisella* and *Vibrio* $TssL_{Cyto}$ sequences. The secondary structures of the EAEC $TssL_{Cyto}$ protein are shown on top whereas conserved residues are shown in red. The residues substituted in this study are indicated by arrowheads (green, cleft; orange, L3-L4 loop; blue, L6-L7 loop). (**B**) Merged crystal structures of the EAEC (PDB: 3U66; green), *Francisella tularensis* (PDB: 4ACL, purple) and *Vibrio cholerae* (PDB: 3V3I, blue) $TssL_{Cyto}$ domains. The positions of the cleft, L3-L4 and L6-L7 loops are indicated by green, orange and blue arrows. (**C-E**) Crystal structures of EAEC (PDB: 3U66; **C**), *Francisella tularensis* (PDB: 4ACL, **D**) and *Vibrio cholerae* (PDB: 3V3I, **E**) $TssL_{Cyto}$ domains. Panel C highlights the positions and locations of the residues substituted, as well as helix αA (loop L3-L4) whereas panel E highlights helices αA (loop L3-L4) and αB (loop L6-L7). The figures were made with Chimera.[56]

Table S1. Strains, Plasmids and Oligonucleotides used in this study.

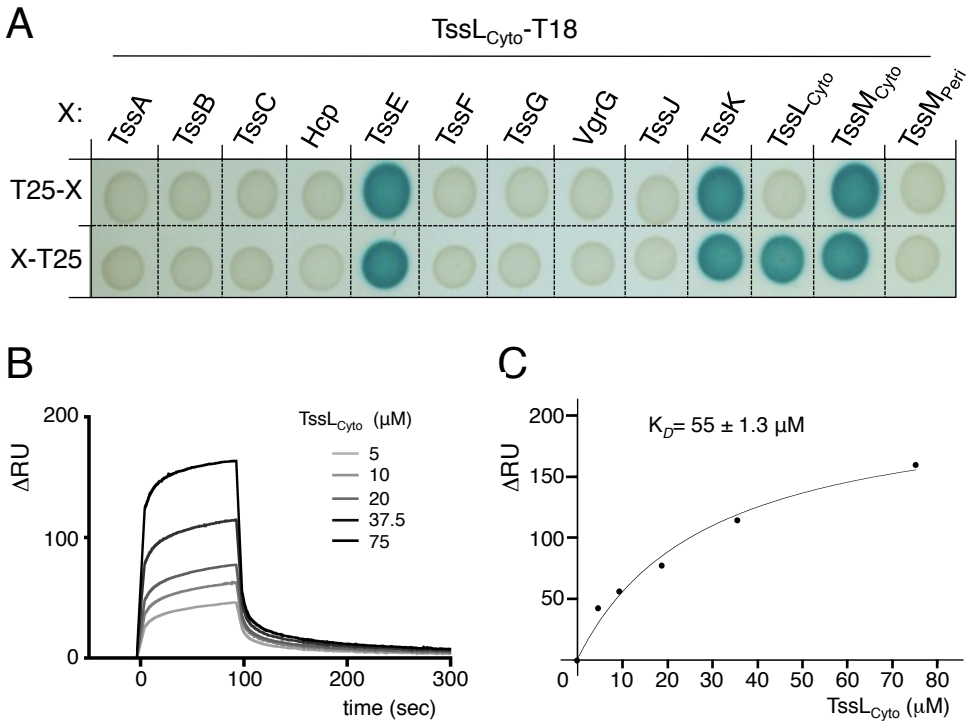

Zoued et al. Figure 1

A

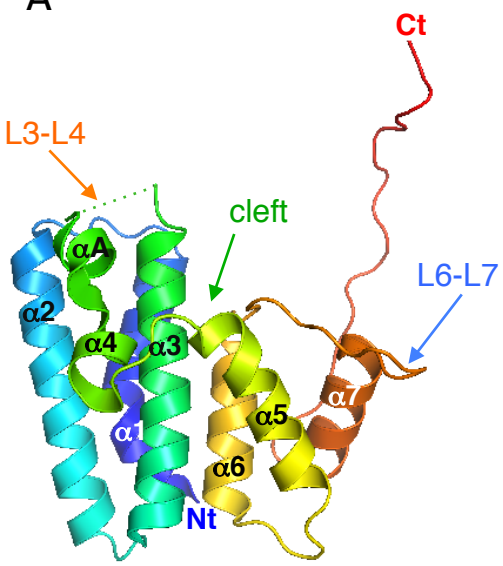

B

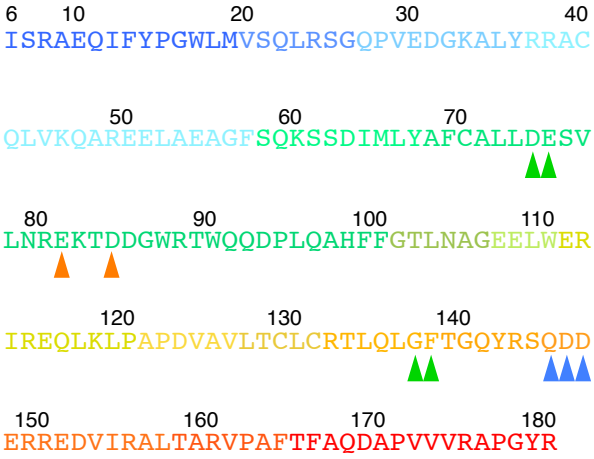

Zoued et al. Figure 2

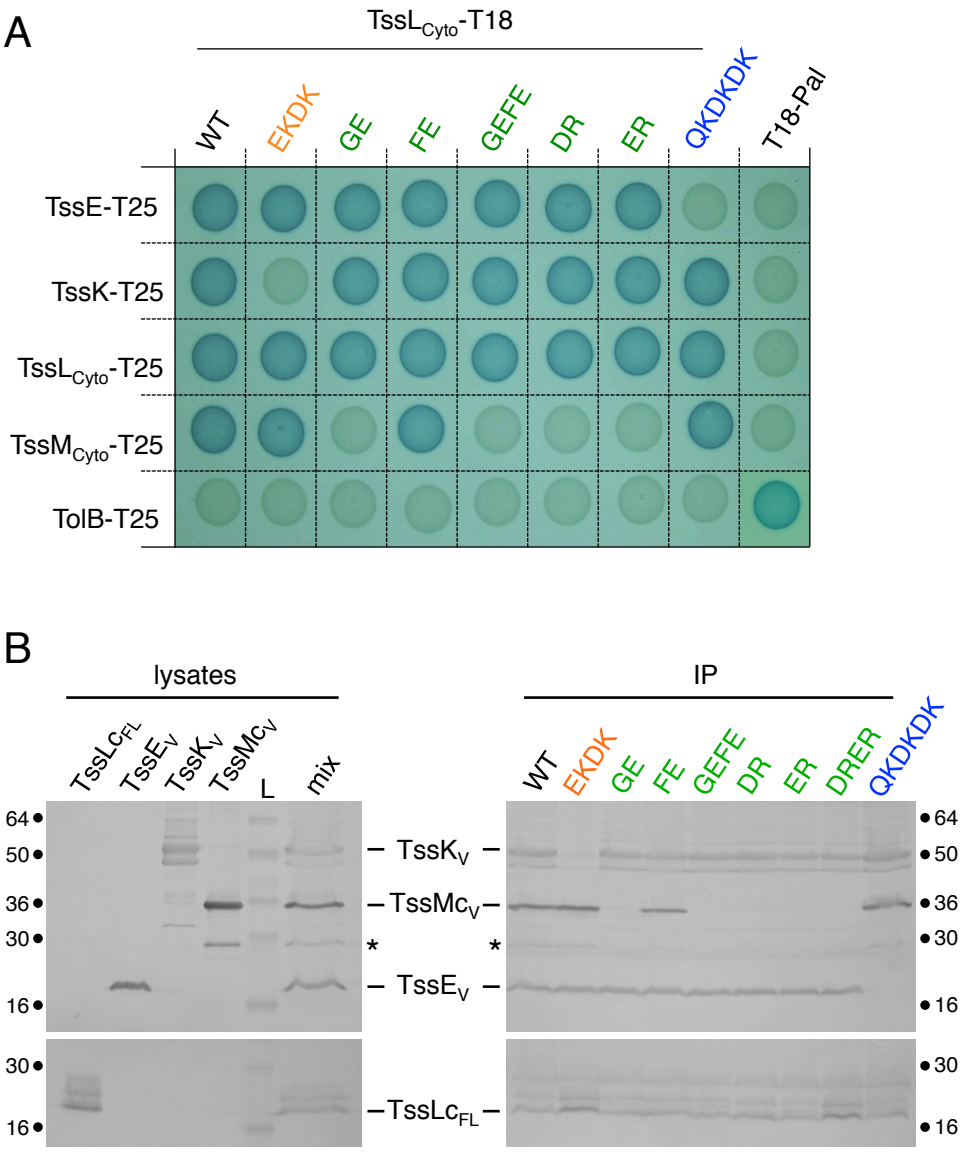

Zoued et al. Figure 3

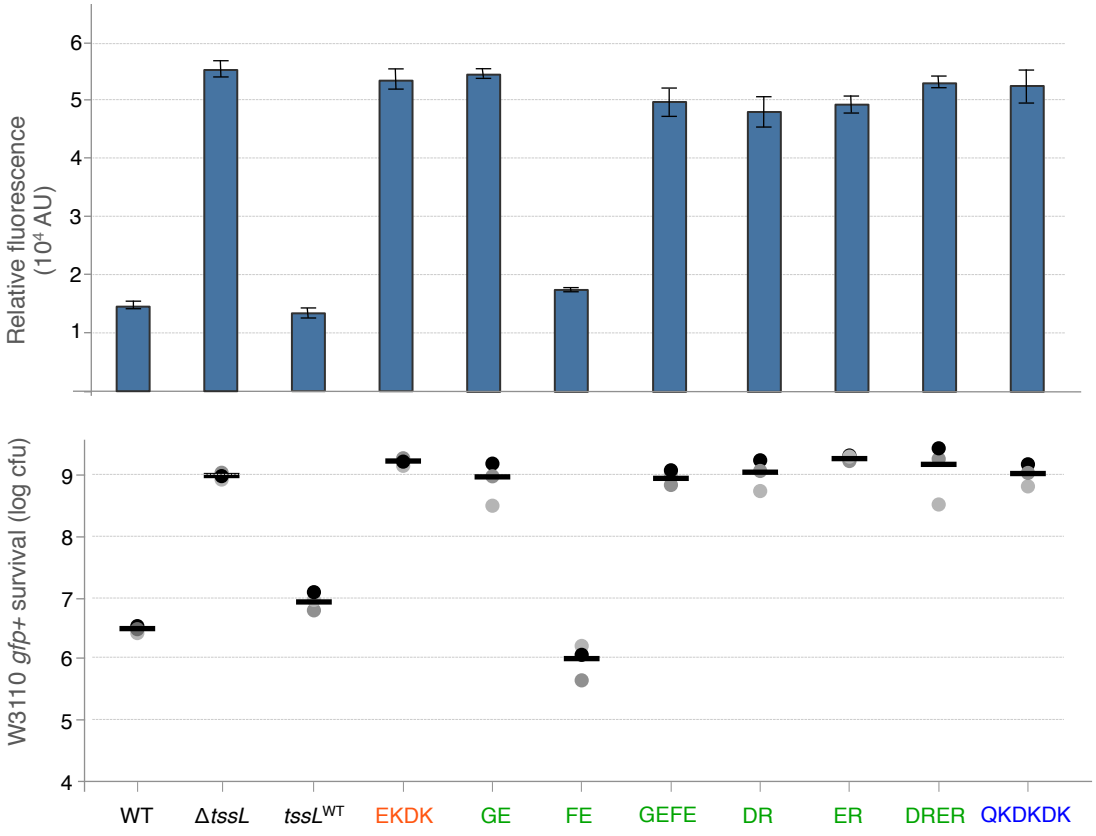

Zoued et al. Figure 4

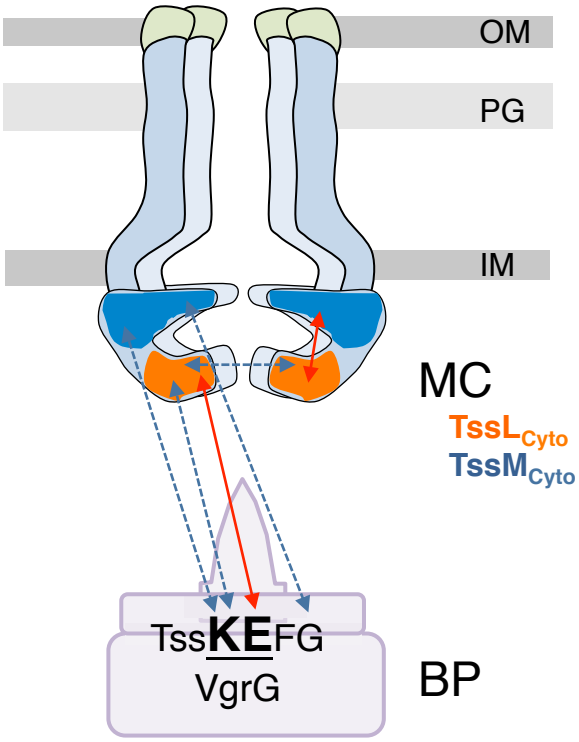

Zoued et al. Figure 5

SUPPLEMENTAL DATA

Structure-function analysis of the TssL cytoplasmic domain reveals a new interaction between the Type VI secretion baseplate and membrane complexes.

A. Zoued, C.J. Cassaro, E. Durand, B. Douzi, A.P. España, C. Cambillau, L. Journet, & E. Cascales

Supplemental Table S1. Strains, plasmids and oligonucleotides used in this study.

Strains

Strains	Description and genotype	Source
E. coli K-12		
DH5α	F-, Δ(*argF-lac*)U169, *phoA*, *supE44*, Δ(lacZ)M15, *relA*, *endA*, *thi*, *hsdR*	New England Biolabs
W3110	F-, lambda- IN(*rrnD-rrnE*)1 *rph*-1	Laboratory collection
BTH101	F-, *cya-99, araD139, galE15, galK16, rpsL1 (Str^R), hsdR2, mcrA1, mcrB1.*	Karimova *et al.*, 2005
BL21(DE3) pLys	F-, miniF *lysY lacI^q* (Cm^R) */ fhuA2 lacZ::T7 gene1 [lon] ompT gal sulA11 R(mcr-73::miniTn10*--Tet^S*)2 [dcm] R(zgb-210::Tn10*-Tet^S*) endA1 Δ(mcrC-mrr) 114::IS10*	New England Biolabs
Enteroaggregative *E. coli*		
17-2	WT enteroaggregative *Escherichia coli*	Arlette Darfeuille-Michaud
17-2Δ*tssL*	17-2 deleted of the *tssL* gene of the *sci1* T6SS gene cluster (EC042_4527)	Aschtgen *et al.*, 2010

Plasmids

Vectors	Description	Source
Expression vectors		
pUA66-*rrnb*	P_{rrnB} *::gfpmut2* transcriptional fusion in pUA66	Zaslaver *et al.*, 2006
pMS600	cloning vector, pOK12 derivative, P15A origin, P*lac*, Kan^R	Aschtgen *et al.*, 2008
pOK-TssL$_{HA}$	*sci1 tssL* (EC042_4527), C-terminal HA tag cloned into pMS600	Aschtgen *et al.*, 2010
pOK-TssL-EKDK	Glu81-to Lys and Asp84-to-Lys substitutions introduced into pOK-TssL$_{HA}$	This study
pOK-TssL-GE	Gly137-to-Glu substitution introduced into pOK-TssL$_{HA}$	This study
pOK-TssL-FE	Phe138-to-Glu substitution introduced into pOK-TssL$_{HA}$	This study

pOK-TssL-GEFE	Gly137-to-Glu and Phe138-to-Glu substitutions introduced into pOK-$TssL_{HA}$	This study
pOK-TssL-DR	Asp74-to-Arg substitution introduced into pOK-$TssL_{HA}$	This study
pOK-TssL-ER	Glu75-to-Arg substitution introduced into pOK-$TssL_{HA}$	This study
pOK-TssL-DRER	Asp74-to-Arg and Glu75-to-Arg substitutions introduced into pOK-$TssL_{HA}$	This study
pOK-TssL-QKDKDK	Gln145-to-Lys, Asp146-to-Lys and Asp147-to-Lys substitutions introduced into pOK-$TssL_{HA}$	This study
pASK-IBA37(+)	cloning vector, f1 origin, P*tet*, Amp^R	IBA technologies
pIBA-$TssLc_{FL}$	*sci1 tssL* cytoplasmic domain (amino-acids 1-184; $TssL_{Cyto}$), C-terminal FLAG tag cloned into pASK-IBA37(+)	Aschtgen *et al.*, 2012
pIBA-$TssL_C$-EKDK	Glu81-to-Lys and Asp84-to-Lys substitutions introduced into pIBA-$TssLc_{FL}$	This study
pIBA-$TssL_C$-GE	Gly137-to-Glu substitution introduced into pIBA-$TssLc_{FL}$	This study
pIBA-$TssL_C$-FE	Phe138-to-Glu substitution introduced into pIBA-$TssLc_{FL}$	This study
pIBA-$TssL_C$-GEFE	Gly137-to-Glu and Phe138-to-Glu substitutions introduced into pIBA-$TssLc_{FL}$	This study
pIBA-$TssL_C$-DR	Asp74-to-Arg substitution introduced into pIBA-$TssLc_{FL}$	This study
pIBA-$TssL_C$-ER	Glu75-to-Arg substitution introduced into pIBA-$TssLc_{FL}$	This study
pIBA-$TssL_C$-DRER	Asp74-to-Arg and Glu75-to-Arg substitutions introduced into pIBA-$TssLc_{FL}$	This study
pIBA-$TssL_C$-QKDKDK	Gln145-to-Lys, Asp146-to-Lys and Asp147-to-Lys substitutions introduced into pIBA-$TssLc_{FL}$	This study
pBAD33	cloning vector, P15A origin, P*ara*, *araC* Cm^R	Guzman *et al.*, 1995
pBAD33-$TssE_{VSV-G}$	*sci1 tssE* (EC042_4545), C-terminal VSV-G tag cloned into pBAD33	This study
pBAD33-$TssK_{VSV-G}$	*sci1 tssK* (EC042_4526), C-terminal VSV-G tag cloned into pBAD33	This study
pBAD33-$TssMc_{VSV-G}$	*sci1 tssM* (EC042_4539) cytoplasmic loop (amino-acids 62-360, $TssM_{Cyto}$), C-terminal VSV-G tag cloned into pBAD33	Laureen Logger
pETG20A	Gateway® expression vector, ColE1 origin, P_{T7}, N-terminal 6xHis-TRX-TEV fusion, Amp^R	Arie Geerlof
pETG20A-$TssL_{Cyto}$	*sci1 tssL* cytoplasmic domain (amino-acids 1-184) cloned into pETG20A	Durand *et al.*, 2012
pETG20A-TssE	*sci1 tssE* cloned into pETG20A	Zoued *et al.*, 2016

Bacterial Two-Hybrid vectors

pT18-FLAG	Bacterial two-hybrid vector, ColE1 origin, P*lac*, T18 fragment of *Bordetella pertussis* CyaA, Amp^R	Battesti & Bouveret, 2008
pT18-Pal	Soluble region of *E. coli* K-12 Pal cloned downstream T18 in pT18-FLAG	Battesti & Bouveret, 2008
pTssL_C-T18	*sci1 tssL* cytoplasmic domain (amino-acids 1-184) cloned upstream T18 into pT18-FLAG	Durand *et al.*, 2012
pTssL_C-EKDK-T18	Glu81-to-Lys and Asp84-to-Lys substitutions introduced into pTssLc-T18	This study
pTssL_C-GE-T18	Gly137-to-Glu substitution introduced into pTssLc-T18	This study
pTssL_C-FE-T18	Phe138-to-Glu substitution introduced into pTssLc-T18	This study
pTssL_C-GEFE-T18	Gly137-to-Glu and Phe138-to-Glu substitutions introduced into pTssLc-T18	This study
pTssL_C-DR-T18	Asp74-to-Arg substitution introduced into pTssLc-T18	This study
pTssL_C-ER-T18	Glu75-to-Arg substitution introduced into pTssLc-T18	This study
pTssL_C-DRER-T18	Asp74-to-Arg and Glu75-to-Arg substitutions introduced into pTssLc-T18	This study
pTssL_C-QKDKDK-T18	Gln145-to-Lys, Asp146-to-Lys and Asp147-to-Lys substitutions introduced into pTssLc-T18	This study
pT25-FLAG	Bacterial two-hybrid vector, P15A origin, P*lac*, T25 fragment of *Bordetella pertussis* CyaA, Kan^R	Battesti & Bouveret, 2008

pTolB-T25	*E. coli* K-12 *tolB* cloned upstream T25 in pT25-FLAG	Battesti & Bouveret, 2008

All others BACTH constructs have been described in Zoued *et al.*, 2013.

Oligonucleotides

Name	Sequence (5' to 3')
For site-directed mutagenesis [a]	
A-TssL-EKDK	ACGAGAGTGTACTGAACCGC**AAA**AAAACA**AAG**GATGGCTGGCGCACCTGGC
B-TssL-EKDK	GCCAGGTGCGCCAGCCATC**CTT**TGTTTT**TTT**GCGGTTCAGTACACTCTCGTC
A-TssL-GE	CTCTGCCGTACGCTTCAGCTC**GAG**TTTACCGGTCAGTACCGGTCGCAG
B-TssL-GE	CTGCGACCGGTACTGACCGGTAAA**CTC**GAGCTGAAGCGTACGGCAGAG
A-TssL-FE	CTCTGCCGTACGCTTCAGCTCGGT**GAG**ACCGGTCAGTACCGGTCGCAG
B-TssL-FE	CTGCGACCGGTACTGACCGGT**CTC**ACCGAGCTGAAGCGTACGGCAGAG
A-TssL-GEFE	CTCTGCCGTACGCTTCAGCTC**GAGGAG**ACCGGTCAGTACCGGTCGCAG
B-TssL-GEFE	CTGCGACCGGTACTGACCGGT**CTCCTC**GAGCTGAAGCGTACGGCAGAG
A-TssL-DR	GTATGCCTTCTGCGCCCTGCTG**CGC**GAGAGTGTACTGAACCGCGAAAAAAC
B-TssL-DR	GTTTTTTCGCGGTTCAGTACACTCTC**GCG**CAGCAGGGCGCAGAAGGCATAC
A-TssL-ER	GTATGCCTTCTGCGCCCTGCTGGAC**CGG**AGTGTACTGAACCGCGAAAAAAC
B-TssL-ER	GTTTTTTCGCGGTTCAGTACACT**CCG**GTCCAGCAGGGCGCAGAAGGCATAC
A-TssL-DRER	GTATGCCTTCTGCGCCCTGCTG**CGCCGG**AGTGTACTGAACCGCGAAAAAAC
B-TssL-DRER	GTTTTTTCGCGGTTCAGTACACT**CCGGCG**CAGCAGGGCGCAGAAGGCATAC
A-TssL-QKDKDK	TTACCGGTCAGTACCGGTCG**AAGAAAAAG**GAGCGTCGCGAAGATGTAATAC
B-TssL-QKDKDK	GTATTACATCTTCGCGACGCTC**CTTTTTCTT**CGACCGGTACTGACCGGTAAAAC

[a] Mutagenized codon in bold

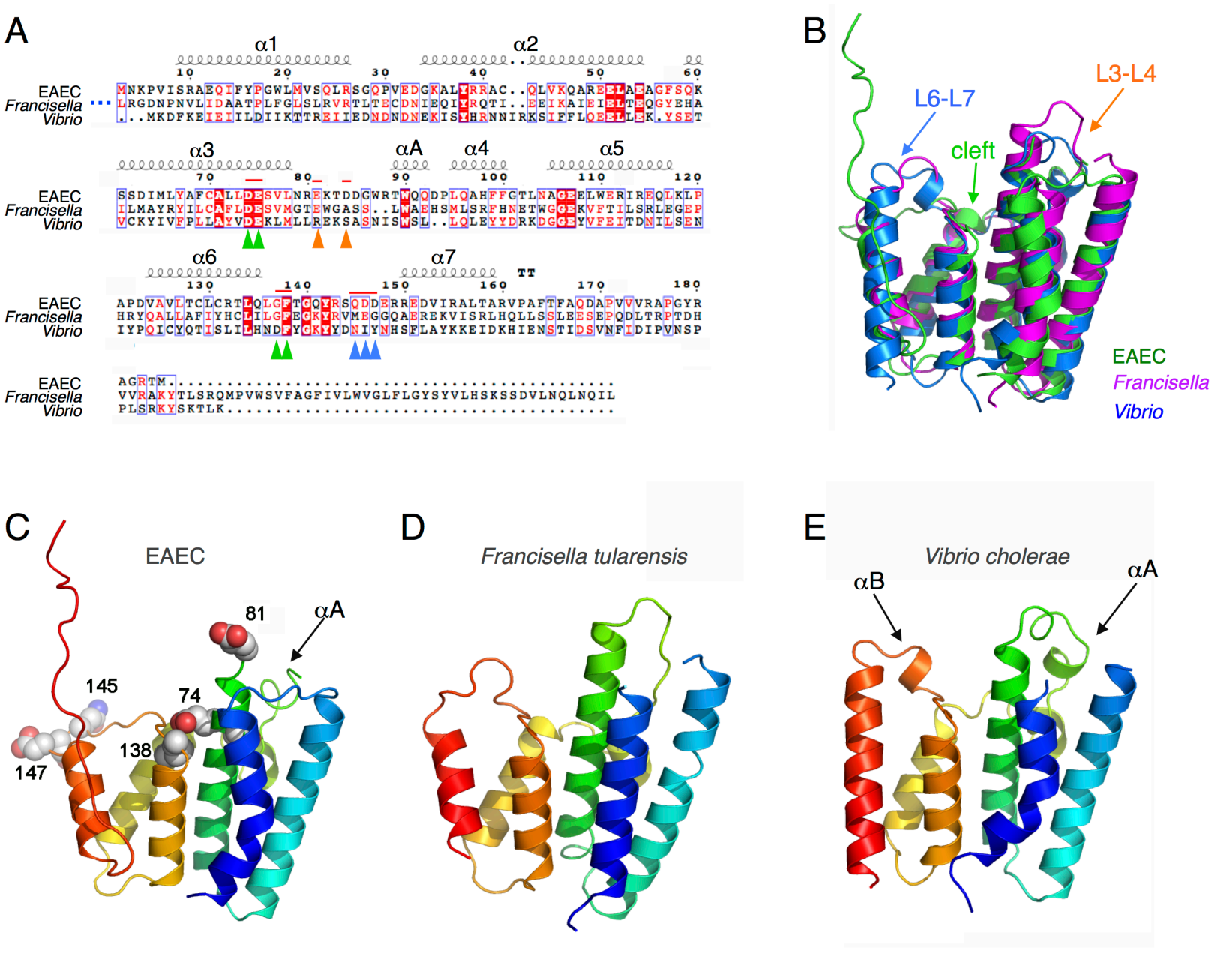
A
α1
α2
α3
αA
α4
α5
α6
α7
EAEC
Francisella
Vibrio
B
L6-L7
L3-L4
cleft
EAEC
Francisella
Vibrio
C
EAEC
81
αA
145
74
138
147
D
Francisella tularensis
E
Vibrio cholerae
αB
αA